Circular polarization switching and bistability in an optically injected 1300 nm spin-VCSEL

S. S. Alharthi[1], A. Hurtado[1,2], V.-M. Korpijarvi[3], M. Guina[3], I. D. Henning[1] and M. J. Adams[1]

[1]*School of Computer Science and Electronic Engineering, University of Essex, Wivenhoe Park, CO4 3SQ, Colchester, United Kingdom*
[2]*Institute of Photonics, Physics Department, University of Strathclyde, Wolfson Centre, 106 Rottenrow East, Glasgow, G4 0NW, Scotland, United Kingdom*
[3]*Optoelectronics Research Centre (ORC), Tampere University of Technology, P.O. Box 692, FIN-33101 Tampere, Finland*
ssmalh@essex.ac.uk

We report the experimental observation of circular polarization switching (PS) and bistability (PB) in a 1300 nm dilute nitride spin-VCSEL. We demonstrate that the circularly polarized optical signal at 1300 nm can gradually or abruptly switch the polarization ellipticity of the spin-VCSEL from right-to-left circular polarization and vice versa. Moreover, different forms of PS and PB between right- and left-circular polarizations are observed by controlling the injection strength and the initial wavelength detuning. These results obtained at the telecom wavelength of 1300nm open the door for novel uses of spin-VCSELs in polarization sensitive applications in future optical systems.

Spin-polarized vertical cavity surface emitting lasers (spin-VCSELs) have been of great interest in recent years due to their functionality and characteristics [1-4]. In such devices, the spin polarized carriers are injected into the active region to create an imbalance in spin-up and spin-down carrier populations that leads to circularly polarized emission. In other words, the information carried by the spin-polarized carriers is converted into circular polarization information carried by the emitted photons. This occurs in accordance with the optical quantum selection rules where the spin angular momentum of the carriers is converted into the angular momentum of the photons. Spin-lasers offer advantages over conventional lasers, such as threshold reduction [1-4], enhanced emission intensities [5-6], increased modulation bandwidth [4][7-9], full polarization controllability [10-13], chirp control [14-15] and ultrafast dynamics [16].

Whilst most work has concentrated on short-wavelength spin-VCSELs [2, 11-12], recently, the first long-wavelength spin-VCSEL emitting at the important telecom wavelength of 1300 nm and operating at room temperature under Continuous Wave (CW) optical pumping has been demonstrated [13]. In that work the polarization of the optical pump showed full controllability over the polarization of the spin-VCSEL [13]. Utilizing such control potentially offers promising applications in spin-dependent switches for optical telecommunications, optical information and data storage, reconfigurable optical interconnects, quantum computing, bandwidth enhancement, encrypted communications and biomedical sensing [5, 17-19].

Optical injection using a linearly polarized coherent external signal into conventional (electrically driven) VCSELs induces novel nonlinear responses which offer additional unique functionality, and performance enhancements leading to a wider range of potential applications [20]. Examples include injection locking [21-23] and a wide range of associated nonlinear dynamics, enhanced modulation bandwidth [22] and new applications such as all-optical memory [24-27], all-optical logic [28-30], signal regeneration [31], microwave and chaotic signal generation [32].

Polarization switching (PS) and its associated polarization bistability (PB) phenomena in conventional VCSELs are interesting consequences of optical injection and can be achieved through linearly polarized optical injection. PS and PB have been experimentally examined under polarized optical injection in conventional VCSELs emitting at short-wavelengths [33-36] and long-wavelengths [37-41]. Polarized optical injection (parallel, orthogonal [42-44] and elliptical [45-47]) has been applied in conventional VCSELs to obtain PS and PB between the two linear and orthogonal polarizations of the device, from parallel to orthogonal polarization and vice versa. However, reports of circularly polarized injection in conventional VCSELs are very limited. Experimentally, we are only aware of one recent work [48] reporting circularly-polarized injection into an 850 nm conventional VCSEL. In complementary studies, theoretical investigations on the effects of different polarized optical injection (elliptical, circular or linear) in conventional VCSELs have been reported by our group [46-47]. Moreover very recently, we have reported the first investigation of an optically-injected dilute nitride spin-VCSEL emitting at the very important telecom wavelength of 1300nm and

operating at room temperature [49-50]. In that work the control of the emitted polarization by the optically injected signal was experimentally and theoretically demonstrated.

Here we report the experimental observation of different forms of (PS) and (PB) induced by circularly polarized optical injection into a 1300nm dilute nitride spin-VCSEL operating at room temperature. The dilute nitride (GaInNAs/GaAs) spin-VCSEL sample used in this work was grown by a solid source molecular beam epitaxy (MBE). The 3-λ cavity of the device consisted of five stacks of three quantum wells (QWs) placed approximately at the antinodes of the standing wave pattern of the optical field. Each 7nm $Ga_{0.67}In_{0.33}N_{0.016}As_{0.984}$ QW was located between 2 nm $Ga_{0.75}In_{0.25}N_{0.017}As_{0.983}$ strain mediating layers. The active region is then enclosed between 16 and 20.5 GaAs/AlAs pairs forming respectively the top and bottom Bragg stacks (with reflectivities estimated as 99.2% and 99.8%).

The optical spectrum and the output-input characteristic of the stand-alone spin-VCSEL can be found in Fig. 1 (b) and (c) of [50], respectively. The experimental setup used to investigate the circular PS and PB in an optically injected spin-VCSEL is also similar to the one reported in Fig. 1 (a) of [50].

In this work to study PS and PB in the 1300 nm dilute nitride spin-VCSEL the initial wavelength detuning ($\Delta\lambda$) between the ML and SL was kept constant while the output polarization ellipticity (ε) of the spin-VCSEL's emission (defined as the ratio between the degree of circular polarization and the total degree of polarization) was measured as a function of increasing and decreasing ML injection power. All the measurements have been conducted when the spin-VCSEL sample was optically pumped to 1.1 times the threshold and injected with a circularly polarized optical signal from the ML. Also, the measurements have been taken for different initial wavelength detunings as will be discussed later. Moreover, two different cases have been analyzed based on interchanging the polarization states of the pump and the ML between right- (RCP) and left-circularly polarized (LCP) states (i.e. when the polarization of the pump is RCP the ML's one is LCP and vice-versa) as will be discussed later.

Fig. 1 illustrates the relationship between the output polarization ellipticity (ε) of the spin-VCSEL and the ML's injection power for different values of initial wavelength detuning. The injection power was measured as the amount of ML's optical power incident on the surface of sample. Results are shown for different negative initial wavelength detunings, -0.50, -0.40, -0.30, -0.20, -0.10, and 0 nm as indicated. Here, the spin-VCSEL was simultaneously pumped with RCP light and optically-injected with an LCP signal from the ML.

Initially, fig. 1 shows a well-known feature of spin-VCSELs whereby its output polarization (ε) is determined by that of the optical pump [13]; then, as

the injected optical power is continuously increased the ML switches the SL's light polarization gradually from almost RCP ($\varepsilon = 0.75$) to almost LCP ($\varepsilon = -0.95$), a behavior that has been recently theoretically [50-51] and experimentally reported [49-50].
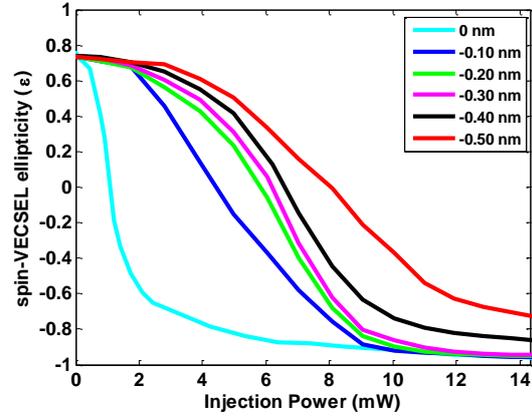

Fig. 1 Output polarization ellipticity (ε) vs injected optical power when the spin-VCSEL is subject to RCP optical pumping and LCP optical injection for negative initial wavelength detunings. Results are plotted for increasing injection strength.

Fig. 1 shows that by changing the initial wavelength detuning from zero to -0.50 nm the lower the negative initial wavelength detuning, the more injection power is needed to achieve the nonlinear gradual PS transition. It should also be mentioned that there was no abrupt PS or PB observed in all the measurements reported in this work for the negative wavelength detuning.
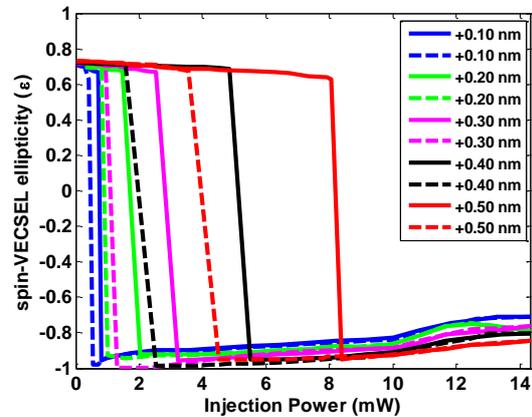

Fig. 2 Output polarization ellipticity (ε) as a function of injection power under RCP optical pump and LCP optical injection for positive values of initial wavelength detuning as indicated. Results are plotted for increasing (solid lines) and decreasing (dashed lines) injection strength values.

Now we will study the effect of increasing and decreasing the injection power of the ML on the output polarization ellipticity of the spin-VCSEL (ε) under the same conditions but for positive initial wavelength detunings ($\Delta\lambda$). Fig. 2 shows the output polarization ellipticity (ε) as a function of increasing and decreasing values of the injection power for different initial wavelength detunings ($\Delta\lambda$), +0.10, +0.20, +0.30, +0.40 and +0.50 nm. Solid and dashed

lines in fig. 2 plot respectively the measured values of ε for increasing and decreasing values of injection strength. In this case, when the initial wavelength was set to a positive value (i.e. 0.10 nm) initially the SL's output ellipticity follows that of the pump and exhibits a value close to RCP emission (ε = 0.75). However, under sufficient injection power (exceeding 700 μW) the LCP ML switches abruptly the SL's polarization from almost RCP (ε = 0.75) to almost LCP (ε = -0.95). On the other hand, when the injection power was decreased back to zero, PS from almost LCP to RCP was observed at a different and lower switching point (560 μW) revealing therefore the existence of circular PB with a clockwise hysteresis cycle in the plane of ε vs. injection power depicted in fig. 2. For higher positive initial wavelength detunings, it has been found that the PS requires more injection power to occur as can be seen for the cases of +0.20, +0.30, +0.40 and +0.50 nm detunings. It is also clear that the width of the hysteresis cycle is dependent on the initial wavelength detuning and injection power. In other words, the higher the initial positive wavelength detuning, the wider is the hysteresis cycle and the more power is required to achieve PS. It is also worth mentioning that for detuning values below +0.10 nm, only gradual PS was observed (as in fig. 1) and no abrupt PS or PB were obtained.
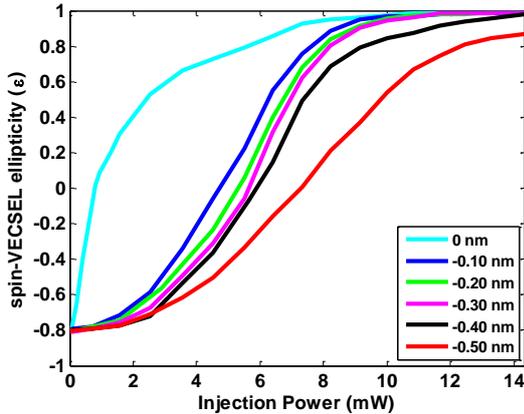

Fig. 3 Output polarization ellipticity (ε) as a function of injection power under LCP optical pump and RCP optical injection for negative initial wavelength detunings. Results are plotted for increasing injection strength values.

In the second case, the polarization of the pump and that of the ML have been interchanged so the spin-VCSEL was subject to LCP optical pumping and RCP optical injection. Fig. 3 plots the relation between the spin-VCSEL output ellipticity (ε) and the injection power for different negative initial wavelength detunings (Δλ), -0.50, -0.40, -0.30, -0.20, -0.10, and 0 nm. As previously mentioned in connection with fig. 1, this figure also shows that, initially, the polarization of the spin-VCSEL is controlled by that of the optical pump (ε = 0.80) when the ML is off and then with increasing power of the ML to higher values, the SL's polarization ellipticity is gradually switched from almost RCP (ε = 0.80) to LCP (ε = -1). Similarly, it can be also seen in fig. 3

that for higher negative wavelength detunings, the spin-VCSEL output ellipticity requires more injection power to switch it gradually to the opposite polarization state. However, the power required to achieve gradual PS in this case (under LCP pumping and RCP injection) is slightly lower than its counterpart in the case of figure 1 (under RCP pumping and LCP injection).
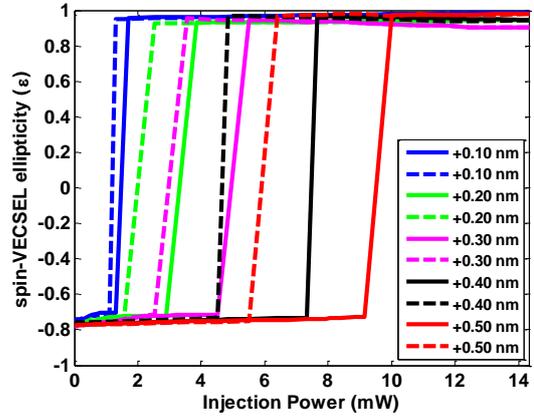

Fig. 4 Output polarization ellipticity (ε) as a function of injection power under LCP optical pump and RCP optical injection for positive initial wavelength detunings. Results are plotted for increasing (solid lines) and decreasing (dashed lines) injection strength values.

The other part of this second case of analysis is shown in Fig. 4. This figure illustrates the variation of ε vs. injection power for positive initial wavelength detunings when the spin-VCSEL was subject to LCP optical pumping and RCP optical injection. Under the same conditions, the measurements were performed at different ML wavelength detuning (Δλ) of, +0.10, +0.20, +0.30, +0.40 and +0.50 nm. The SL's behavior in this case is almost identical to the one shown in fig. 2. For example when (Δλ) was set to +0.10 nm, starting with the injection strength at zero, the polarization of the pump controls that of the SL for low enough injection power whereas for higher values of injection (above 1.7 mW) the control of the SL's polarization passed from the pump to the ML. This was also accompanied by abrupt PS from almost LCP (ε = -0.80) to RCP (ε = +1). Moreover, decreasing the injection power back to zero caused PS from RCP to LCP at a lower and different injection value (1.29 mW). This demonstrates the existence of PB with anticlockwise hysteresis cycle as illustrated in fig. 4. This figure shows that the width of the nonlinear hysteresis cycle and PB transition changes as the initial wavelength detuning is increased for higher positive values. It can be also noted that the required injection power to achieve abrupt PS for positive wavelength detuning increases with increased initial detuning. However, the minimum injection power to achieve abrupt PS in this case (1.7 mW) is slightly higher than in the case of fig. 2 (700 μW, under RCP pumping and LCP injection). Moreover, PS below +0.10 nm initial wavelength detuning takes place

gradually, similar to the PS in the negative detuning side, and neither abrupt PS nor PB were observed.

In summary, this contribution reports the experimental observation of optical power circular polarization switching (PS) and polarization bistability (PB) in a 1300 nm spin-VCSEL subject to circularly polarized external optical injection. The relationships between output polarization ellipticity and optical power variations have been experimentally analyzed using different polarization states for pump and injection. Different forms of circular PS, gradual and abrupt, in addition to different forms of PB, anticlockwise and clockwise, have been experimentally observed. This diversity of behavior in a spin-VCSEL at the important telecom wavelength of 1300 nm and operated at room temperature offers promise for novel uses of spin lasers in optical signal processing, optical switching and optical interconnection applications, such as all-optical inversion and all-optical signal regeneration, in long-haul optical networks.

Acknowledgements

References

[1] J. Rudolph, D. Hägele, H. M. Gibbs, G. Khitrova, and M. Oestreich, Appl. Phys. Lett. 82, 4516 (2003).

[2] J. Rudolph, S. Dohrmann, D. Hagele, M. Oestreich, and W. Stolz, Appl. Phys. Lett. 87, 241117 (2005).

[3] D. Basu, D. Saha, and P. Bhattacharya, Phys. Rev. Lett. 102, 093904 (2009).

[4] J. Lee, S. Bearden, E. Wasner, and I. Zutic, Appl. Phys. Lett. 105 (4), 042411 (2014).

[5] M. Holub, J. Shin, D. Saha, and P. Bhattacharya, Phys. Rev. Lett. 98,146603 (2007).

[6] D. Basu, D. Saha, C. C. Wu, M. Holub, Z. Mi, and P. Bhattacharya, Appl. Phys. Lett. 92, 091119 (2008).

[7] N. C. Gerhardt, M. Y. Li, H. Jahme, H. Hopfner, T. Ackermann, and M. R. Hofmann, Appl. Phys. Lett. 99, 151107 (2011).

[8] J. Lee, W. Falls, R. Oszwaldowski, and I. Zutic´, Appl. Phys. Lett. 97, 041116 (2010).

[9] H. Hopfner, M. Lindemann, N. C. Gerhardt, and M. R. Hofmann, Appl.Phys. Lett. 104, 022409 (2014).

[10] H. Ando, T. Sogawa, and H. Gotoh, Appl. Phys. Lett. 73, 566 (1998).

[11] N. Gerhardt, S. Hovel, M. Hofmann, J. Yang, D. Reuter, and A. Wieck, Electron. Lett., 42, 2,88 (2006).

[12] S. Hovel, A. Bischoff, N. C. Gerhardt, M. R. Hofmann, T. Ackemann, A. Kroner, and R. Michalzik, Appl. Phys. Lett. 92, 041118 (2008).

[13] K. Schires, R. Al Seyab, A. Hurtado, V.-M. Korpijärvi, M. Guina, I. D. Henning, and M. J. Adams, Opt. Exp., 20, 4, 3550 (2012).

[14] J. Lee, R. Oszwałdowski, C. Gøthgen, and I. Zutic, Phys. Rev. B 85, 045314 (2012).

[15] G. Boeris, J. Lee, K. Vyborny, and I. Zutic, Appl. Phys. Lett. 100, 121111 (2012).

[16] N. C. Gerhardt, H. Höpfner, M. Lindemann, M. R. Hofmann, Proc. SPIE 9167, 916703 (2014)

[17] N. C. Gerhardt and M. R. Hofmann, Adv. Opt. Technol. 2012, 268949 (2012).

[18] J. Sinova and I. Žutić, Nature Mater. 11, pp.368-371 (2012).

[19] K. Ikeda, T. Fujimoto, H. Fujino, and T. Katayama, IEEE Photon. Technol. Lett., 21, 18, pp. 1350–1352 (2009)

[20] S. Wieczorek, B. Krauskopf, T. B. Simpson, and D. Lenstra, Phys. Rep. 416, 1 (2005).

[21] C.-H. Chang, L. Chrostowski, and C. J. Chang-Hasnain, IEEE J. Select. Topics Quantum Electron., 9, 5, pp. 1386–1393, (2003).

[22] L. Chrostowski, B. Faraji, W. Hofmann, M.-C. Amann, S. Wieczorek, and W. W. Chow, IEEE J. Sel. Topics Quantum Electron., 13, 5, pp. 1200–1208, (2007).

[23] A. Hurtado, D. Labukhin, I. D. Henning, and M. J. Adams, IEEE J. Sel. Top. Quantum Electron. 15, 3, 585 (2009).

[24] J. Sakaguchi, T. Katayama, and H. Kawaguchi, Opt. Exp., 18, 1212362 (2010).

[25] T. Katayama, T. Ooi, and H. Kawaguchi, IEEE J. Quantum Electron., 45, 11, 1495 (2009).

[26] J. Sakaguchi, T. Katayama, and H. Kawaguchi, IEEE J. Quantum Electron., 46, 11, 1526 (2010).

[27] S. H. Lee, H. W. Jung, K. H. Kim, M. H. Lee, B. S. Yoo, J. Roh, and K. A. Shore, IEEE Photon. Technol. Lett., 22, 23, 1759 (2010).

[28] Y. Onishi, N. Nishiyama, C. Caneau, F. Koyama, and C. E. Zah, IEEE J. Select. Topics Quantum Electron. , 11, 5, 999 (2005).

[29] K. Hasebe and F. Koyama, Jap. J. Appl. Phys. Lett., 45, 8B, 6697 (2006).

[30] C. F. Marki, S. Moro, D. R. Jorgesen, P. Wen, and S. C. Esener, Electron. Lett. 44, 4, 292 (2008).

[31] Y. Onishi and F. Koyama, IEICE Trans. Electron., E87C, 3, 409 (2004).

[32] A. Quirce and A. Valle, Opt. Exp., 20, 13390 (2012).

[33] Z. G. Pan, S. Jiang, M. Dagenais, R. A. Morgan, M. Kojima, M. T. Asom, and R. E. Leibenguth, Appl. Phys. Lett., 63, 22,2999 (1993).

[34] J. Buesa Alt´es, I. Gatare, K. Panajotov, H. Thienpont, and M. Sciamanna, IEEE J. Quantum Electron., 42, 2, 198 (2006).

[35] Y. Hong, K. A. Shore, A. Larsson, M. Ghisoni, and J. Halonen, IEE Proc. Optoelectron.,148, 1, 31 (2001).

[36] I. Gatare, J. Buesa, H. Thienpont, K. Panajotov, and M. Sciamanna, Opt. Quantum Electron. 38, 4-6, 429 (2006).

[37] A. Valle, M. Gomez-Molina, and L. Pesquera, IEEE J. Sel. Top Quantum Electron.,14, 3, 895 (2008).

[38] A. Hurtado, I. D. Henning, and M. J. Adams, IEEE J. Sel. Top. Quantum Electron., 14, 3, 911 (2008).

[39] K. H. Jeong, K. H. Kim, S. H. Lee, M. H. Lee, B. S. Yoo, and K. A. Shore, IEEE Photon. Technol. Lett., 20, 9–12, 779 (2008).

[40] A. Hurtado, A. Quirce, A. Valle, L. Pesquera, and M. J. Adams, Opt. Express., 17, 26, 23637 (2009).

[41] A. Hurtado, I. D. Henning, and M. J. Adams, Opt. Lett, 34, 3, 365 (2009).

[42] A. Valle, M. Sciamanna, and K. Panajotov, IEEE J. Quantum Electron., 44, 2, 136 (2008).

[43] A. Hurtado, A. Quirce, A. Valle, L. Pesquera, and M. J. Adams, Opt. Exp.,18, 9, 9423 (2010).

[44] K. Schires, A. Hurtado, I. D. Henning, and M. J. Adams, AIP Advances,1, 3, 032131 (2011).

[45] R. Al Seyab, K. Schires, N. Khan, A. Hurtado, I. D. Henning, and M. J. Adams, IEEE J. Sel. Topics Quantum Electron.,17, 5, 1242 (2011).

[46] R. Al-Seyab, K. Schires, A. Hurtado, and I. Henning, M. Adams. Conference (ISLC 2012), San Diego, CA, USA (2012).

[47] R. Al Seyab, K. Schires, A. Hurtado, I. D. Henning, and M. J. Adams, IEEE J. Select. Topics Quantum Electron., 19, 4 , 1700512 (2013).

[48] A. A. Qader, Y. Hong and K. A. Shore, J. Lightwave Technol., 29, 24, 3804 (2011).

[49] Sami Alharthi, Antonio Hurtado, Ville-Markus Korpijärvi, Mircea Guina, Ian Hening, Michael Adams, Conference on Lasers and Electro-Optics (CLEO), San Jose, CA, USA, SF1G (2014).

[50] S.S. Alharthi, A. Hurtado, R.K. Al Seyab, V.-M. Korpijarvi, M. Guina, I.D. Henning and M.J. Adams, Accepted for publication in Appl. Phys. Lett., 105(18), 181106 (2014).

[51] R. Al-Seyab, Ph.D thesis, University of Essex, UK (2012).